SCIENTIFIC REPORTS
nature research

OPEN

Mitochondrial Unfolded Protein Response to Microgravity Stress in Nematode *Caenorhabditis elegans*

Peidang Liu, Dan Li, Wenjie Li & Dayong Wang*

Caenorhabditis elegans **is useful for assessing biological effects of spaceflight and simulated microgravity. The molecular response of organisms to simulated microgravity is still largely unclear. Mitochondrial unfolded protein response (mt UPR) mediates a protective response against toxicity from environmental exposure in nematodes. Using HSP-6 and HSP-60 as markers of mt UPR, we observed a significant activation of mt UPR in simulated microgravity exposed nematodes. The increase in HSP-6 and HSP-60 expression mediated a protective response against toxicity of simulated microgravity. In simulated microgravity treated nematodes, mitochondria-localized ATP-binding cassette protein HAF-1 and homeodomain-containing transcriptional factor DVE-1 regulated the mt UPR activation. In the intestine, a signaling cascade of HAF-1/DVE-1-HSP-6/60 was required for control of toxicity of simulated microgravity. Therefore, our data suggested the important role of mt UPR activation against the toxicity of simulated microgravity in organisms.**

During the spaceflight, the significant risk on movement, muscle, and metabolism of human beings and animals have been frequently observed[1–5]. Microgravity contributes to the detected pathological alterations during spaceflight[1,4]. Simulated microgravity treatment is an important strategy to predict the possible toxicity of microgravity and to elucidate the underlying mechanisms. The simulated microgravity can also result in the abnormal psychological performance, endocrine, and intestinal dysfunction as observed by microgravity during the spaceflight[6–9].

Nematode *Caenorhabditis elegans*, a classic model animal, is a wonderful model for toxicological study of stresses or toxicants[10–14]. *C. elegans* is a suitable model for assessing effects of microgravity[15,16]. With the work in "the first International *C. elegans* Experiment in Space" (ICE-First) experiments as an example, it has been observed that microgravity could potentially at least cause the toxicity on early embryogenesis, muscle development, germline development, locomotion behavior, and reproduction in nematodes[17–23]. The toxicity of simulated microgravity on nematodes could be further assessed more recently[24–27]. The observed toxicity induced by simulated microgravity was under the control of insulin and p38 mitogen-activated protein kinase (MAPK) signaling pathways in nematodes[24,26].

In the mitochondrion, mitochondrial unfolded protein response (mt UPR) mediates a protective response against the toxicity from environmental stresses or toxicants in nematodes[28]. However, the response of mt UPR signaling to simulated microgravity remains largely unclear. We here examined the induction of mt UPR in simulated microgravity treated nematodes and the underlying mechanism. Our data demonstrated the noticeable activation of mt UPR in simulated microgravity treated nematodes. Moreover, the mtUPR signaling was involved in the regulation of response to simulated microgravity.

Results

Simulated microgravity induced the mt UPR in nematodes. In nematodes, HSP-60 and HSP-6 are mt UPR markers[29,30]. Simulated microgravity treatment (24-h) caused a significant increase in expression of both *hsp-6* and *hsp-60* (Fig. 1a). HSP-6 can be expressed in intestinal cells[31]. Meanwhile, using the transgenic strain of *zcIs13*[HSP-6::GFP], we found an obvious increase in HSP-6::GFP expression in the intestine of nematodes treated with simulated microgravity (Fig. 1b).

Effect of RNAi knockdown of *hsp-6* or *hsp-60* on toxicity of simulated microgravity. We detected the more severe induction of intestinal reactive oxygen species (ROS) production and decrease in locomotion behavior in simulated microgravity treated *hsp-6(RNAi)* or *hsp-60(RNAi)* nematodes compared with those in

Medical School, Southeast University, Nanjing, 210009, China. *email: dayongw@seu.edu.cn

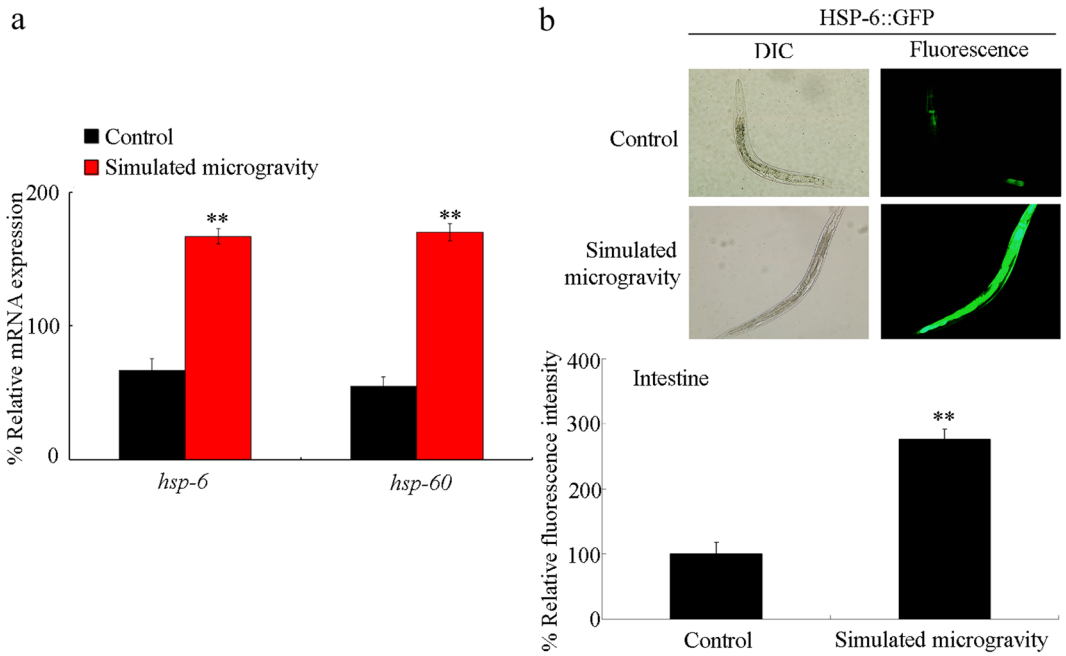

Figure 1. Simulated microgravity treatment induced the mt UPR in nematodes. (**a**) Effect of simulated microgravity treatment on expression of *hsp-6* and *hsp-60*. Relative expression ratio between the examined genes and the reference gene (*tba-1*) was determined. (**b**) Effect of simulated microgravity treatment on expression of intestinal HSP-6::GFP. DIC, differential interference contrast. Simulated microgravity treatment was performed for 24-h. Bars represent means ± SD. $^{**}P < 0.01$ *vs* Control.

simulated microgravity treated wild-type nematodes (Fig. 2). Thus, RNAi knockdown of *hsp-6* or *hsp-60* induced a susceptibility to toxicity of simulated microgravity.

HAF-1 and DVE-1 were involved in the regulation of response to simulated microgravity. In nematodes, some proteins, such as ATFS-1, DVE-1, UBL-5, HAF-1, CLPP-1, and LIN-65, are required for mt UPR induction by regulating the expression of mt UPR markers during the stress response[32–35]. Simulated microgravity treatment (24-h) caused a significant increase in expressions of *haf-1* and *dve-1* (Fig. 3a). We did not observe the significant alteration in expression of other genes in simulated microgravity treated nematodes (Fig. 3b).

We further found that RNAi knockdown of *haf-1* or *dve-1* induced the more severe toxicity of simulated microgravity in inducing intestinal ROS production and in decreasing locomotion behavior compared with those in wild-type nematodes (Fig. 3b,c), suggesting that the nematodes with RNAi knockdown of *haf-1* or *dve-1* were susceptible to the toxicity of simulated microgravity.

Intestine-specific activity of HAF-1, DVE-1, HSP-6, or HSP-60 in regulating the response to simulated microgravity. In nematodes, intestinal insulin and p38 MAPK signaling pathways play a crucial function in regulating the response to simulated microgravity[24,26]. We next focused on the intestine to determine the activity of HAF-1, DEV-1, HSP-6, and HSP-60 in regulating simulated microgravity toxicity. Simulated microgravity treatment significantly increased the expressions of *haf-1*, *dve-1*, *hsp-6*, and *hsp-60* in isolated intestines (Fig. S1). After the simulated microgravity treatment, intestine-specific RNAi knockdown of *haf-1*, *dev-1*, *hsp-6*, or *hsp-60* resulted in a more severe intestinal ROS production compared with VP303 nematodes (Fig. 4a), suggesting the susceptibility of nematodes with intestine-specific RNAi knockdown of *haf-1*, *dev-1*, *hsp-6*, or *hsp-60* to simulated microgravity toxicity. Since the VP303 nematodes has defect in locomotion behavior, we did not further investigate locomotion behavior phenotypes.

Genetic interaction of HSP-6/60 with HAF-1 or DVE-1 in regulating the response to simulated microgravity. To determine the interaction of HSP-6/HSP-60 with HAF-1 or DEV-1 in regulating the response to simulated microgravity, transgenic strain overexpressing intestinal HAF-1 or DEV-1 was generated. Under the condition without the simulated microgravity treatment, the nematodes overexpressing intestinal HAF-1 or DEV-1 do not show obvious intestinal ROS production (Fig. 4b). Intestinal overexpression of HAF-1 or DEV-1 suppressed the toxicity of simulated microgravity in inducing intestinal ROS production, demonstrating the resistance of nematodes overexpressing intestinal HAF-1 or DEV-1 to simulated microgravity toxicity (Fig. 4b). Moreover, RNAi knockdown of *hsp-6* or *hsp-60* effectively inhibited the resistance of nematodes overexpressing intestinal HAF-1 or DEV-1 to the toxicity of simulated microgravity in inducing intestinal ROS production (Fig. 4b). Therefore, HSP-6/60 acted downstream of intestinal HAF-1 or DEV-1 to regulate the response to simulated microgravity.

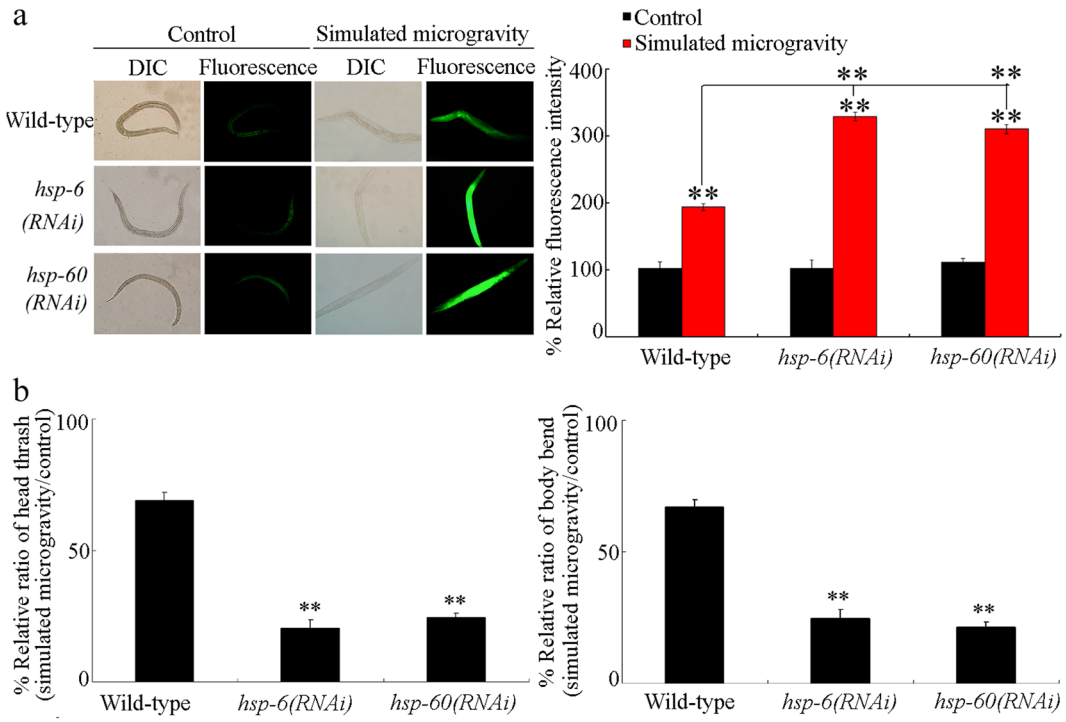

Figure 2. RNAi knockdown of *hsp-6* or *hsp-60* induced a susceptibility to the toxicity of simulated microgravity. (**a**) RNAi knockdown of *hsp-6* or *hsp-60* caused a susceptibility to the toxicity of simulated microgravity in inducing intestinal ROS production. DIC, differential interference contrast. Bars represent means ± SD. $^{**}P < 0.01$ *vs* Control (if not specially indicated). (**b**) RNAi knockdown of *hsp-6* or *hsp-60* caused a susceptibility to the toxicity of simulated microgravity in decreasing locomotion behavior. Considering that the examined nematodes have deficit in locomotion behavior, the locomotion behavior was expressed as the ratio between simulated microgravity and control. Bars represent means ± SD. $^{**}P < 0.01$ *vs* Wild-type. Simulated microgravity treatment was performed for 24-h.

HAF-1 and DVE-1 regulated the mt UPR activation in simulated microgravity treated nematodes. To confirm the function of HAF-1 and DVE-1 in modulating mt UPR activation in simulated microgravity treated nematodes, we carried our RNAi knockdown of *haf-1* or *dve-1* in *zcIs13*[HSP-6::GFP] nematodes. RNAi knockdown of *haf-1* or *dve-1* obviously suppressed the activation of HSP-6::GFP induced by simulated microgravity (Fig. 5a), suggesting the requirement of HAF-1 and DVE-1 for the mt UPR activation in simulated microgravity treated nematodes.

p38 MAPK signaling pathway was not involved in the regulation of mt UPR activation in simulated microgravity treated nematodes. Our previous study has raised an intestinal cascade of NSY-1-SEK-1-PMK-1-ATF-7/SKN-1 required for the control of simulated microgravity toxicity in nematodes[24]. Nevertheless, we found that RNAi knockdown of *nsy-1*, *sek-1*, *pmk-1*, *atf-7*, or *skn-1* in the p38 MAPK signaling pathway did not obviously influence HSP-6::GFP induction in simulated microgravity treated nematodes (Fig. 5b), which suggests that the p38 MAPK signaling pathway did not regulate the mt UPR activation induced by simulated microgravity.

Effect of intestinal RNAi knockdown of *hsp-6* or *hsp-60* on mitochondrial dysfunction, mitochondrial ROS production, and mitophagy in simulated microgravity treated nematodes. We used the oxygen consumption rate and mitochondrial membrane potential to reflect the mitochondrial function, and found that simulated microgravity treatment could significantly decrease the oxygen consumption ratio and reduce the mitochondrial membrane potential (Fig. S2a,b). Meanwhile, treatment with simulated microgravity induced the significant mitochondrial ROS production (Fig. S2c). We employed *dct-1* and *pink-1* as molecular markers of mitophagy in nematodes[36]. Simulated microgravity treatment induced the significant increase in expression of both *dct-1* and *pink-1* in nematodes (Fig. S2d).

Moreover, we observed that intestinal RNAi knockdown of *hsp-6* or *hsp-60* induced the more severe decrease in oxygen consumption ratio and reduction in mitochondrial membrane potential compared with VP303 nematodes after simulated microgravity treatment (Fig. S2a,b). In simulated microgravity treated VP303 nematodes, intestinal RNAi knockdown of *hsp-6* or *hsp-60* caused the more severe induction of mitochondrial ROS production (Fig. S2c). Furthermore, intestinal RNAi knockdown of *hsp-6* or *hsp-60* significantly suppressed the increase in expressions of both *dct-1* and *pink-1* induced by simulated microgravity treatment (Fig. S2d).

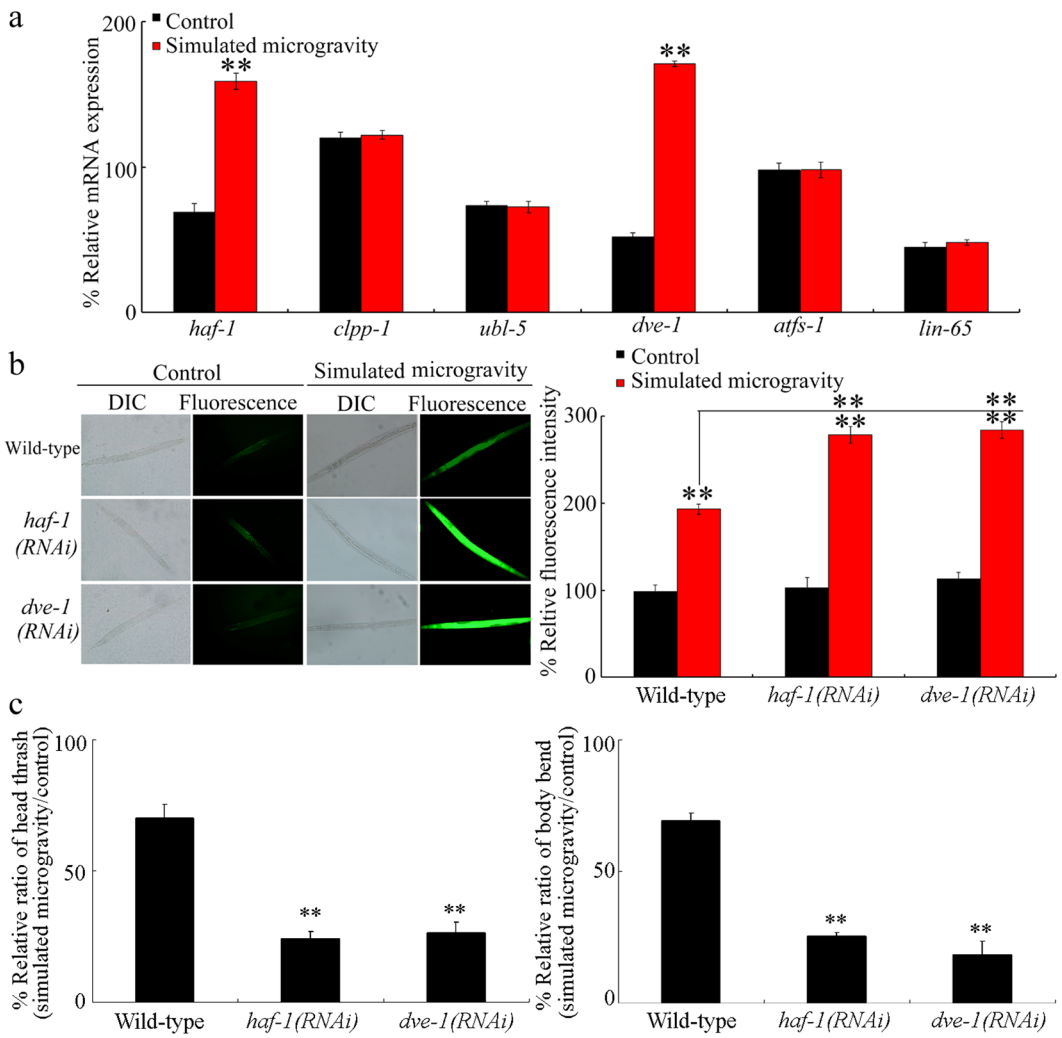

Figure 3. HAF-1 and DVE-1 were involved in the control of response to simulated microgravity. (**a**) Effect of simulated microgravity on expressions of *haf-1*, *clpp-1*, *ubl-5*, *dev-1*, *atfs-1*, and *lin-65*. Relative expression ratio between the examined genes and the reference gene (*tba-1*) was determined. Bars represent means ± SD. $^{**}P < 0.01$ *vs* Control. (**b**) RNAi knockdown of *haf-1* or *dve-1* induced a susceptibility to toxicity of simulated microgravity in inducing intestinal ROS production. DIC, differential interference contrast. Bars represent means ± SD. $^{**}P < 0.01$ *vs* Control (if not specially indicated). (**c**) RNAi knockdown of *haf-1* or *dve-1* induced a susceptibility to toxicity of simulated microgravity in decreasing locomotion behavior. Considering that the examined nematodes have deficit in locomotion behavior, the locomotion behavior was expressed as the ratio between simulated microgravity and control. Bars represent means ± SD. $^{**}P < 0.01$ *vs* Wild-type. Simulated microgravity treatment was performed for 24-h.

Discussion

Using HSP-6 and HSP-60 as the mt UPR markers, the significant induction in expression of HSP-6 and HSP-60 was observed in simulated microgravity treated nematodes (Fig. 1). This observation demonstrated the potential noticeable induction of mt UPR by simulated microgravity in organisms. Simulated microgravity also induced the mitochondrial dysfunction in rat cerebral arteries[37]. Thus, simulated microgravity may at least activate two different responses in mitochondrion of organisms. One is the mitochondrial dysfunction, and another is the mt UPR activation.

We further found that RNAi knockdown of *hsp-6* or *hsp-60* could induce a susceptibility to simulated microgravity toxicity (Fig. 2), which indicated that the induction of HSP-6 or HSP-60 mediates a protective mt UPR response to simulated microgravity. The microgravity also potentially induced the proteomics changes involved in endoplasmic reticulum (ER) response[38,39]. That is, both mt UPR and ER UPR may be potentially activated by simulated microgravity treatment in organisms.

During the control of mt UPR, mitochondria-localized ATP-binding cassette protein HAF-1 governs export of peptides from matrix, which is required for mt UPR signaling across mitochondrial inner membrane[35]. Mitochondrial matrix protease CLPP-1 mediates the generation of peptides in mitochondrial matrix[34,35]. The mt UPR activation correlates with the nuclear redistribution of transcriptional factor DVE-1, and complex formation

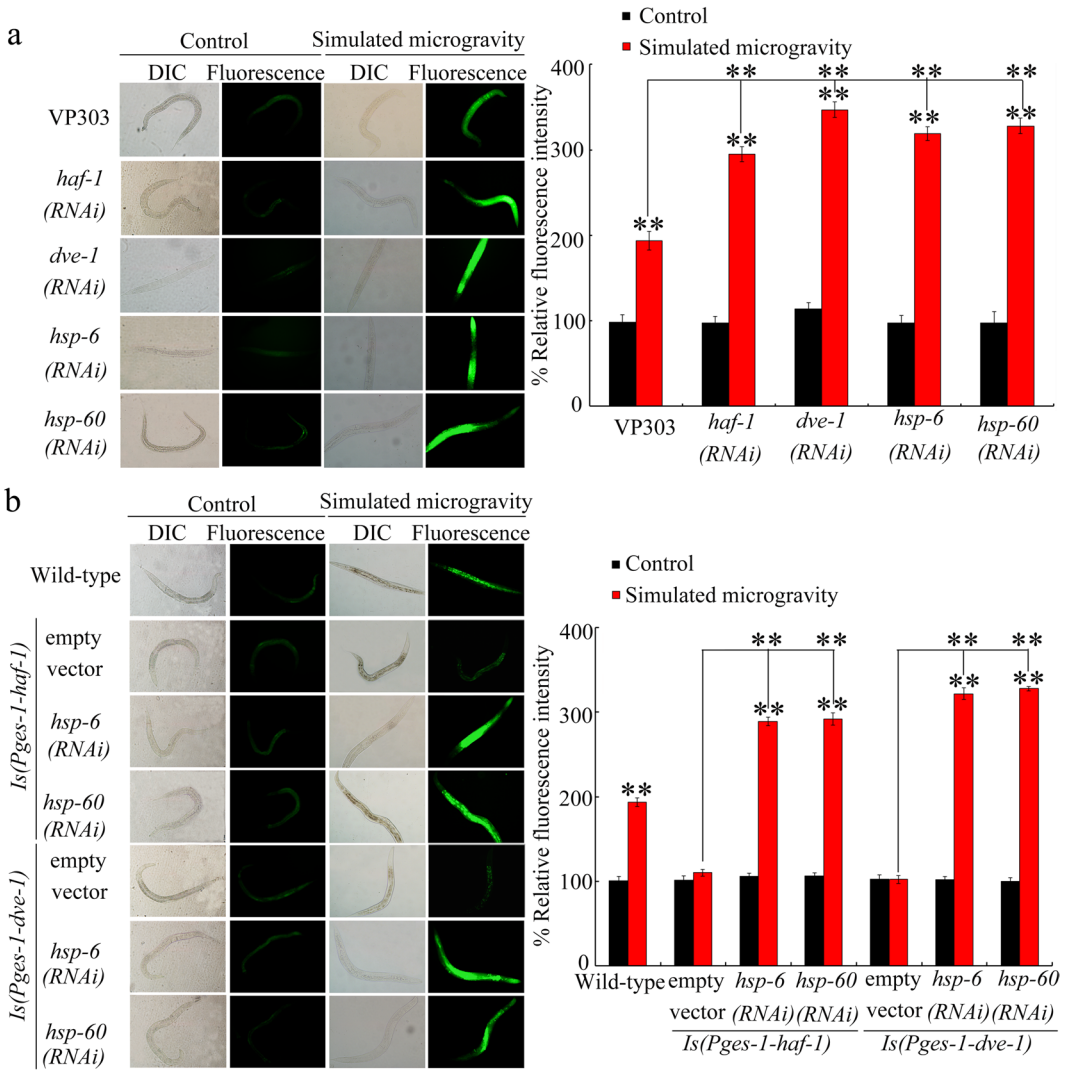

Figure 4. Intestine-specific activity of mt UPR related genes in regulating the toxicity of simulated microgravity. (**a**) Effect of RNAi knockdown of *haf-1*, *dev-1*, *hsp-6*, or *hsp-60* on toxicity of simulated microgravity in inducing intestinal ROS production. (**b**) Effect of RNAi knockdown of *hsp-6* or *hsp-60* on intestinal ROS production in simulated microgravity treated nematodes with intestinal overexpression of HAF-1 or DVE-1. DIC, differential interference contrast. Empty vector, L4440. Bars represent means ± SD. $^{**}P < 0.01$ *vs* Control (if not specially indicated). Simulated microgravity treatment was performed for 24-h.

between DVE-1 and small ubiquitin-like protein UBL-5[34]. Mitochondrial import efficiency of another transcriptional factor ATFS-1 is also required for mt UPR activation[33]. The mt UPR activation also requires nuclear co-factor LIN-65[32]. Among the genes encoding these proteins, we found that simulated microgravity only affected expressions of *haf-1* and *dve-1* (Fig. 3a). This observation suggested that simulated microgravity may only affect activity of transcriptional factor DVE-1, but not influence the activities of another transcriptional factor ATFS-1 and nuclear co-factor LIN-65. Additionally, in the complex of DVE-1-UBL-5, simulated microgravity may be not able to influence activity of UBL-5. During the activation of mt UPR, simulated microgravity may affect export process of peptides from the matrix controlled by HAF-1, but not influence the CLPP-1-mediated generation of peptides in mitochondrial matrix. HSP-6 is an ortholog of human HSP70, HSP-60 is an ortholog of human HSP60, HAF-1 is an ortholog of human ABCB10, and DVE-1 is an ortholog of human STAB2. It was reported that the simulated microgravity could upregulate the expressions of HSP60 and HSP70 in human bone stem cells[40].

The functional analysis further confirmed the involvement of HAF-1 and DVE-1 in regulating the response to simulated microgravity (Fig. 3b,c). Our previous studies have suggested that oxidative stress-related, insulin, and p38 MAPK signaling pathways were required for toxicity induction of simulated microgravity in nematodes[24,26,41]. Our data further suggests the involvement of mt UPR signaling pathway in regulating the response to simulated microgravity.

We further provide the evidence to indicate the intestine-specific activity of HAF-1, DEV-1, HSP-6, and HSP-60 in modulating the response to simulated microgravity (Fig. 4a). That is, besides insulin and p38 MAPK

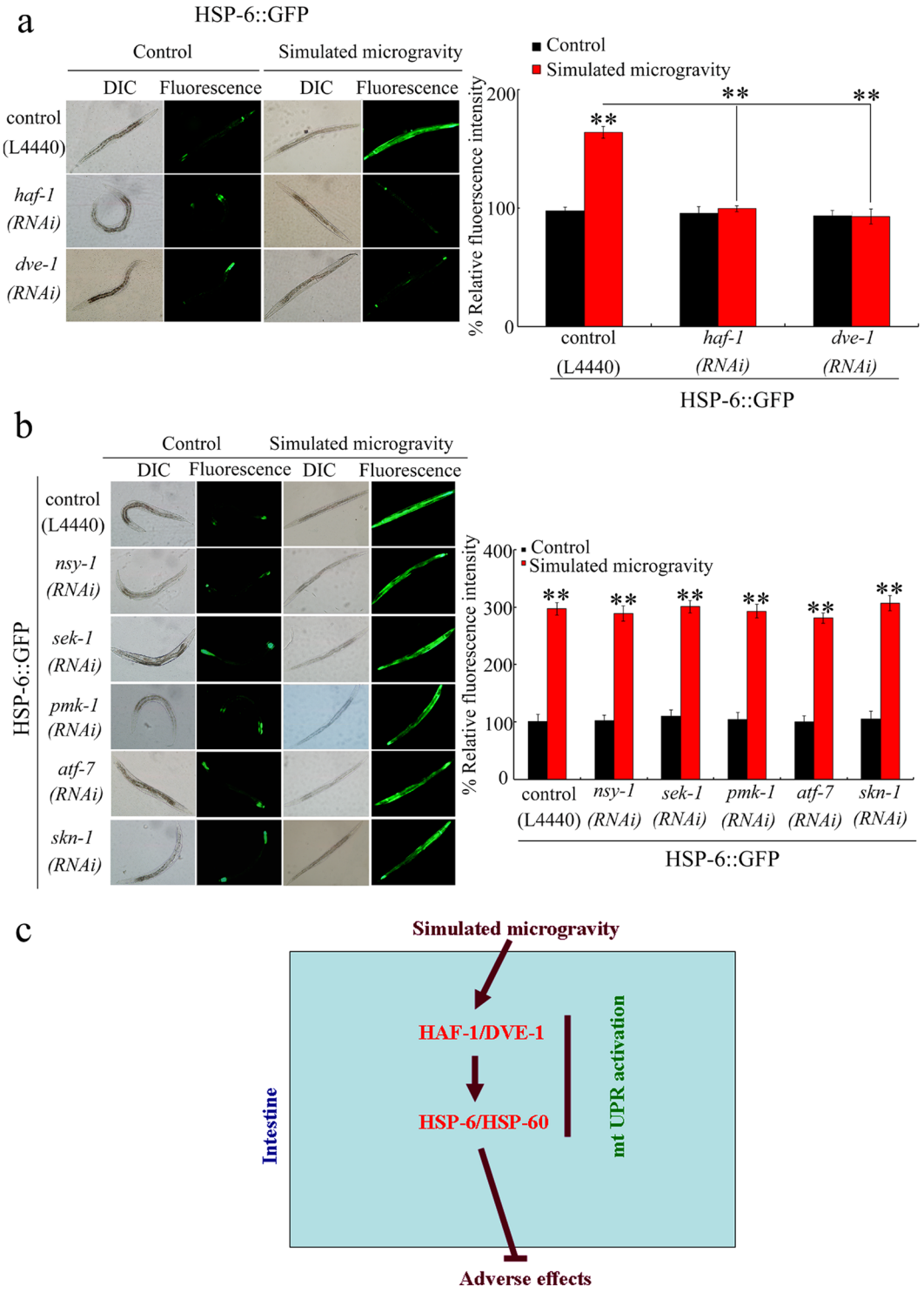

Figure 5. RNAi knockdown of *haf-1* or *dev-1* regulated the mt UPR in simulated microgravity treated nematodes. (**a**) Effect of RNAi knockdown of *haf-1* or *dev-1* on HSP-6::GFP induction in simulated microgravity treated nematodes. (**b**) Effect of RNAi knockdown of *nsy-1*, *sek-1*, *pmk-1*, *atf-7*, or *skn-1* on HSP-6::GFP induction in simulated microgravity treated nematodes. DIC, differential interference contrast. Empty vector, L4440. Simulated microgravity treatment was performed for 24-h. Bars represent means ± SD. $^{**}P < 0.01$ *vs* Control (if not specially indicated). (**c**) A diagram showing the role of mt UPR signaling pathway in regulating the response to simulated microgravity in nematodes.

signaling pathways, mt UPR signaling also acted in the intestine to regulate the response to simulated microgravity. We further raised an intestinal signaling cascade of HAF-1/DEV-1-HSP-6/60 required for the regulation of response to simulated microgravity (Fig. 4b). Nevertheless, p38 MAPK signaling pathway was not required for

the activation of mt UPR induced by simulated microgravity (Fig. 5b). However, RNAi knockdown of *haf-1* or *dve-1* inhibited the activation of mt UPR induced by simulated microgravity (Fig. 5a). Therefore, mt UPR and p38 MAPK signaling may mediate two different molecular responses to simulated microgravity in nematodes.

In this study, we further found that the mt UPR activation was associated with induction of mitochondrial dysfunction, mitochondrial ROS production, and mitophagy in simulated microgravity treated nematodes. After simulated microgravity treatment, we detected the decrease in oxygen consumption ratio (Fig. S2a), the reduction in mitochondrial membrane potential (Fig. S2b), the induction of mitochondrial ROS production (Fig. S2c), and the activation of mitophagy (Fig. S2d). Moreover, our data suggested that the mt UPR signaling may regulate mitochondrial dysfunction, mitochondrial ROS production, and mitophagy in simulated microgravity treated nematodes. We detected the more severe decrease in oxygen consumption ratio, reduction in mitochondrial membrane potential, and induction of mitochondrial ROS production in *hsp-6(RNAi)* or *hsp-60(RNAi)* nematodes compared with VP303 after simulated microgravity treatment (Fig. S2a–c). Additionally, RNAi knodown of *hsp-6* or *hsp-60* suppressed the mitophagy activation induced by simulated microgravity (Fig. S2d).

Together, we examined the mt UPR activation induced by simulated microgravity in nematodes. We detected a significant activation of mt UPR in nematodes treated with simulated microgravity. The increase in expressions of HSP-6 and HSP-60 mediated a protective response to simulated microgravity. In simulated microgravity treated nematodes, HAF-1 and DEV-1 regulated the activation of mt UPR. Moreover, we raised an intestinal signaling cascade of HAF-1/DEV-1-HSP-6/60 involved in the regulation of response to simulated microgravity (Fig. 5c). These findings highlight the crucial protective function of mt UPR activation against the toxicity of simulated microgravity in organisms.

Methods

Simulated microgravity. Simulated microgravity was performed as described[26]. Young adults (approximately 100 young adults) were suspended in a soft and movable agar medium (0.2%, half filled) in chamber of Rotary System^{TM} (Synthecon). Balancing sedimentation-induced gravity by centrifugation (horizontally at 30 rpm for 24 h) was carried out to generate the simulated microgravity[42]. Control young adults were maintained in 0.2% agar medium without microgravity treatment.

Animal maintenance. Transgenic strains (VP303/*kbIs7[nhx-2p::rde-1]* and SJ4100/*zcIs13*[HSP-6::GFP]) and wild-type N2 were used in this study. Animals were maintained normally on nematode growth medium (NGM) plates as described[43]. VP303 is used for intestine-specific RNA interference (RNAi) knockdown of certain gene[44]. NGM plates were fed with food for nematodes, *Escherichia coli* OP50. Bleaching mixture (2% HOCl, 0.45 M NaOH) was used to treat the gravid nematodes in order to collect eggs and to prepare age synchronous L1-larvae or young adults.

Intestinal ROS production. ROS production was used to reflect the activation of oxidative stress[45]. ROS production was examined as described[46]. Nematodes were labeled using 1 μM CM-H_2DCFDA for 3 h in the darkness. The nematodes were analyzed for the excitation wavelength at 488 nm and the emission filter at 510 nm under a laser scanning confocal microscope. Relative ROS signal fluorescence intensity was semi-quantified in relative to the total protein concentration. Fifty nematodes were analyzed per treatment.

Locomotion behavior. Locomotion behaviors were used to reflect the functional state of motor neurons[47]. Locomotion behavior was examined based on two endpoints (head thrash and body bend) as described[48]. A change for bending direction at body mid-region of nematodes has been recorded as a head thrash. The head thrash was analyzed in 1 min. A change of posterior bulb direction has been recorded as a body bend. The body bend was analyzed in 20 sec. Considering that some the nematodes with RNAi knockdown of certain gene (such as *haf-1* or *dve-1*) required for the control of mt UPR have deficit in locomotion behavior, the locomotion behavior was expressed as the ratio between simulated microgravity and control. Forty nematodes were analyzed per treatment.

Quantitative real-time polymerase chain reaction (qRT-PCR). The reagent of Trizol (Invitrogen) was used to extract the RNAs. Using ABI 7500 real-time PCR system with Evagreen (Biotium), qRT-PCR was performed to analyze the expression of genes required for the mt UPR activation. Transcriptional expression ratio between genes required for the mt UPR and reference gene (*tba-1*) was determined. Biological reactions were carried out for three times. Table S1 shows the primer information.

RNAi. The L1-larvae were fed with HT115 (*E. coli* strain) carrying double-stranded RNA corresponding to certain gene(s)[49]. Once the L1 larvae on RNAi plates became the gravid animals, they were picked on fresh RNAi plate to lay eggs. The second generation was used for simulated microgravity treatment. HT115 bacteria expressing empty vector L4440 was selected as a negative control. Efficiency of RNAi was confirmed by qRT-PCR (data not shown).

DNA construction. PCR was performed using genomic DNA to amply intestine-specific *ges-1* promoter. *haf-1* or *dve-1* cDNA fragment was subcloned into pPD_95_77 vector carrying the *ges-1* promoter. Gene transformation was performed by coinjecting 10–40 μg/mL testing DNA and 60 μg/mL marker DNA (*Pdop-1::rfp*) into the gonad[50]. Table S2 shows the related primer information.

Oxygen consumption rate. The oxygen consumption rate was measured as described[51]. After microgravity treatment, the examined nematodes were washed with M9 buffer for three times. The nematodes were then

diluted to 500 worms per 50 ml and incubated in Mitocell chamber. The slopes of linear portions of plots were used to assess the oxygen consumption rates. Three independent trials were performed.

Mitochondrial membrane potential. Tetramethylrhodamine ethyl ester (TMRE) uptake was used to measure the mitochondrial membrane potential[52]. After microgravity treatment, the examined nematodes were washed with M9 buffer for three times. The nematodes were then labeled with TMRE (0.1 μM) for 24-h. Relative TMRE fluorescence intensity was examined under a laser scanning confocal microscope. Fifty nematodes were analyzed per treatment.

Mitochondrial ROS production. After microgravity treatment, the examined nematodes were washed with M9 buffer for three times. To determine the mitochondrial ROS production, the nematodes were labeled with 0.5 μM MitoTracker®Red CM H2XRos for 48-h[53]. Relative fluorescence intensity was examined under a laser scanning confocal microscope. Fifty nematodes were analyzed per treatment.

Statistical analysis. SPSS 12.0 software was used for statistical analysis. One-way analysis of variance (ANOVA) was used to analyze the differences between groups. Two-way ANOVA analysis was used for the examination of multiple factor comparison. Probability level of 0.01 (**) was considered to be statistically significant.

Received: 23 August 2019; Accepted: 24 October 2019;
Published online: 11 November 2019

References

1. Steinberg, F., Kalicinski, M., Dalecki, M. & Bock, O. Human performance in a realistic instrument-control task during short-term microgravity. *PLoS ONE* **10**, e0128992 (2015).
2. Fitts, R. H. *et al*. Prolonged space flight-induced alterations in the structure and function of human skeletal muscle fibres. *J. Physiol.* **588**, 3567–3592 (2010).
3. Altman, P. L. & Talbot, J. M. Nutrition and metabolism in spaceflight. *J. Nutr.* **117**, 421–427 (1987).
4. Longnecker, D. E., Manning, F. J. & Worth, M. H. Jr. (eds). Review of NASA's Longitudinal Study of Astronaut Health. Washington, The National Academic Press (2004).
5. Seibert, F. S. *et al*. The effect of microgravity on central aortic blood pressure. *Am. J. Hypertension* **31**, 1183–1189 (2018).
6. Feuerecker, M. *et al*. Headache under simulated microgravity is related to endocrine, fluid distribution, and tight junction changes. *Pain* **157**, 1072–1078 (2016).
7. Prakash, M. *et al*. Microgravity simulated by the 6 head-down tilt bed rest test increases intestinal motility but fails to induce gastrointestinal symptoms of space motion sickness. *Dig. Dis. Sci.* **60**, 3053–3061 (2015).
8. Li, P. *et al*. Simulated microgravity disrupts intestinal homeostasis and increases colitis susceptibility. *FASEB J.* **29**, 3263–3273 (2015).
9. Chouker, A. *et al*. Simulated microgravity, psychic stress, and immune cells in men: observations during 120-day 6° HDT. *J. Appl. Physiol.* **90**, 1736–1743 (2001).
10. Wang, D.-Y. Nanotoxicology in *Caenorhabditis elegans*. Springer Nature Singapore Pte Ltd. (2018).
11. Leung, M. C. *et al*. *Caenorhabditis elegans*: an emerging model in biomedical and environmental toxicology. *Toxicol. Sci.* **106**, 5–28 (2008).
12. Qu, M. *et al*. Exposure to MPA-capped CdTe quantum dots causes reproductive toxicity effects by affecting oogenesis in nematode *Caenorhabditis elegans*. *Ecotoxicol. Environ. Safety* **173**, 54–62 (2019).
13. Liu, P.-D. *et al*. Dysregulation of neuronal Gαo signaling by graphene oxide in nematode *Caenorhabditis elegans*. *Sci. Rep.* **9**, 6026 (2019).
14. Shi, L.-F. *et al*. A circular RNA *circ_0000115* in response to graphene oxide in nematodes. *RSC Adv.* **9**, 13722–13735 (2019).
15. Gao, Y., Xu, D., Zhao, L. & Sun, Y. The DNA damage response of *C. elegans* affected by gravity sensing and radiosensitivity during the Shenzhou-8 spaceflight. *Mutat. Res.* **795**, 15–26 (2017).
16. Zhao, L., Gao, Y., Mi, D. & Sun, Y. Mining potential biomarkers associated with space flight in *Caenorhabditis elegans* experienced Shenzhou-8 mission with multiple feature selection techniques. *Mutat. Res.* **791-792**, 27–34 (2016).
17. Higashitani, A. *et al*. Checkpoint and physiological apoptosis in germ cells proceeds normally in spaceflown *Caenorhabditis elegans*. *Apoptosis* **10**, 949–954 (2005).
18. Sasagawa, Y. *et al*. Effects of gravity on early embryogenesis in *Caenorhabditis elegans*. *Biol. Sci. Space* **17**, 217–218 (2003).
19. Higashibata, A. *et al*. Microgravity elicits reproducible alterations in cytoskeletal and metabolic gene and protein expression in space-flown *Caenorhabditis elegans*. *NPG Microgravity* **2**, 15022 (2016).
20. Szewczyk, N. J. *et al*. *Caenorhabditis elegans* survives atmospheric breakup of STS-107, space shuttle Columbia. *Astrobiology* **5**, 690–705 (2005).
21. Higashibata, A. *et al*. Decreased expression of myogenic transcriptional factors and myosin heavy chains in *Caenorhabditis elegans* muscles developed during spaceflight. *J. Exp. Biol.* **209**, 3209–3218 (2006).
22. Adachi, R. *et al*. Spaceflight results in increase of thick filament but bot thin filament proteins in the paramyosin mutant of *Caenorhabditis elegans*. *Adv. Space Res.* **41**, 816–823 (2008).
23. Adenle, A. A., Johnsen, B. & Szewczyk, N. J. Review of the results from the International *C. elegans* first experiment (ICE-FIRST). *Adv. Space Res.* **44**, 210–216 (2009).
24. Li, W.-J., Wang, D.-Y. & Wang, D.-Y. Regulation of the response of *Caenorhabditis elegans* to simulated microgravity by p38 mitogen-activated protein kinase signaling. *Sci. Rep.* **8**, 857 (2018).
25. Tee, L. F. *et al*. Effects of simulated microgravity on gene expression and biological phenotypes of a single generation *Caenorhabditis elegans* cultured on 2 different media. *Life Sci. Space Res.* **15**, 11–17 (2017).
26. Kong, Y., Liu, H.-L., Li, W.-J. & Wang, D.-Y. Intestine-specific activity of insulin signaling pathway in response to microgravity stress in *Caenorhabditis elegans*. *Biochem. Biophys. Res. Commun.* **517**, 278–284 (2019).
27. Liu, H. –L., Guo, D. –Q., Kong, Y., Rui, Q & Wang, D. -Y. Damage on functional state of intestinal barrier by microgravity stress in nematode *Caenorhabditis elegans*. *Ecotoxicol. Environ. Safety*, https://doi.org/10.1016/j.ecoenv.2019.109554 (2019).
28. Wang, D.-Y. Molecular Toxicology in *Caenorhabditis elegans*. Springer Nature Singapore Pte Ltd. (2019).
29. Pellegrino, M. W. *et al*. Mitochondrial UPR-regulated innate immunity provides resistance to pathogen infection. *Nature* **516**, 414–417 (2014).
30. Melber, A. & Haynes, C. M. UPR^{mt} regulation and output: a stress response mediated by mitochondrial-nuclear communication. *Cell Res.* **28**, 281–295 (2018).
31. Sanders, J., Scholz, M., Merutka, I. & Biron, D. Distinct unfolded protein responses mitigate or mediate effects of nonlethal deprivation of *C. elegans* sleep in different tissues. *BMC Biol.* **15**, 67 (2017).

32. Tian, Y. *et al*. Mitochondrial stress induces chromatin reorganization to promote longevity and UPR(mt). *Cell* **165**, 1197–1208 (2016).
33. Nargund, A. M., Pellegrino, M. W., Fiorese, C. J., Baker, B. M. & Haynes, C. M. Mitochondrial import efficiency of ATFS-1 regulates mitochondrial UPR activation. *Science* **337**, 587–590 (2012).
34. Haynes, C. M., Petrova, K., Benedetti, C., Yang, Y. & Ron, D. ClpP mediates activation of a mitochondrial unfolded protein response in *C. elegans*. *Dev. Cell* **13**, 467–480 (2007).
35. Haynes, C. M., Yang, Y., Blais, S. P., Neubert, T. A. & Ron, D. The matrix peptide exporter HAF-1 signals a mitochondrial UPR by activating the transcription factor ZC376.7 in *C. elegans*. *Mol. Cell* **37**, 529–540 (2010).
36. D'Amico, D. *et al*. The RNA-binding protein PUM2 impairs mitochondrial dynamics and mitophagy during aging. *Mol. Cell* **73**, 775–787 (2019).
37. Zhang, R. *et al*. Simulated microgravity-induced mitochondrial dysfunction in rat cerebral arteries. *FASEB J.* **28**, 2715–2724 (2014).
38. Feger, B. J. *et al*. Microgravity induces proteomics changes involved in endoplasmic reticulum stress and mitochondrial protection. *Sci. Rep.* **6**, 34091 (2016).
39. Zupanska, A. K., LeFrois, C., Ferl, R. J. & Paul, A. L. HSFA2 functions in the physiological adaptation of undifferentiated plant cells to spaceflight. *Int. J. Mol. Sci.* **20**, E390 (2019).
40. Cazzaniga, A., Maier, J. A. M. & Castiglioni, S. Impact of simulated microgravity on human bone stem cells: new hints for space medicine. *Biochem. Biophys. Res. Commun.* **473**, 181–186 (2016).
41. Zhao, L., Rui, Q. & Wang, D.-Y. Molecular basis for oxidative stress induced by simulated microgravity in nematode *Caenorhabditis elegans*. *Sci. Total Environ.* **607-608**, 1381–1390 (2017).
42. Khaoustov, V. I. *et al*. Induction of three-dimensional assembly of human liver cells by simulated microgravity. *In Vitro Cell. Dev. Biol. Anim.* **35**, 501–509 (1999).
43. Brenner, S. Genetics of *Caenorhabditis elegans*. *Genetics* **77**, 71–94 (1974).
44. Zhao, Y.-L., Jin, L., Wang, Y., Kong, Y. & Wang, D.-Y. Prolonged exposure to multi-walled carbon nanotubes dysregulates intestinal *mir-35* and its direct target MAB-3 in nematode *Caenorhabditis elegans*. *Sci. Rep.* **9**, 12144 (2019).
45. Liu, P.-D., Shao, H.-M., Kong, Y. & Wang, D.-Y. Effect of graphene oxide exposure on intestinal Wnt signaling in nematode *Caenorhabditis elegans*. *J. Environ. Sci.* https://doi.org/10.1016/j.jes.2019.09.002 (2019).
46. Qu, M. *et al*. Nanopolystyrene at predicted environmental concentration enhances microcystin-LR toxicity by inducing intestinal damage in *Caenorhabditis elegans*. *Ecotoxicol. Environ. Safety*, https://doi.org/10.1016/j.ecoenv.2019.109568 (2019).
47. Qu, M., Kong, Y., Yuan, Y.-J. & Wang, D.-Y. Neuronal damage induced by nanopolystyrene particles in nematode *Caenorhabditis elegans*. *Environ. Sci.: Nano* **6**, 2591–2601 (2019).
48. Qu, M., Luo, L. –B., Yang, Y. –H., Kong, Y. & Wang, D.-Y. Nanopolystyrene-induced microRNAs response in *Caenorhabditis elegans* after long-term and lose-dose exposure. *Sci. Total Environ*. https://doi.org/10.1016/j.scitotenv.2019.134131 (2019).
49. Qu, M., Qiu, Y. -X, Kong, Y. & Wang, D. -Y. Amino modification enhances reproductive toxicity of nanopolystyrene on gonad development and reproductive capacity in nematode *Caenorhabditis elegans*. *Environ. Pollut.*, https://doi.org/10.1016/j.envpol.2019.112978 (2019).
50. Mello, C. & Fire, A. DNA transformation. *Methods Cell Biol* **48**, 451–482 (1995).
51. Chen, P., Hsiao, K. & Chou, C. Molecular characterization of toxicity mechanism of single-walled carbon nanotubes. *Biomaterials* **34**, 5661–5669 (2013).
52. Zuryn, S., Kuang, J. & Ebert, P. Mitochondrial modulation of phosphine toxicity and resistance in *Caenorhabditis elegans*. *Toxicol. Sci.* **102**, 179–186 (2008).
53. Civelek, M., Mehrkens, J., Carstens, N., Fitzenberger, E. & Wenzel, U. Inhibition of mitophagy decreases survival of *Caenorhabditis elegans* by increasing protein aggregation. *Mol. Cell. Biochem.* **452**, 123–131 (2019).

Acknowledgements

This work was supported by the grant from National Natural Science Foundation of China (No. 81771980).

Author contributions

D. Wang designed the research. P. Liu, D. Li and W. Li performed the experiments. D. Wang wrote the paper.

Competing interests

The authors declare no competing interests.

Additional information

Supplementary information is available for this paper at https://doi.org/10.1038/s41598-019-53004-9.

Correspondence and requests for materials should be addressed to D.W.

Reprints and permissions information is available at www.nature.com/reprints.

Publisher's note Springer Nature remains neutral with regard to jurisdictional claims in published maps and institutional affiliations.